MOLECULAR AND CELLULAR BIOLOGY, July 2004, p. 5733–5745 Vol. 24, No. 13
0270-7306/04/$08.00+0 DOI: 10.1128/MCB.24.13.5733–5745.2004


# The Transcription Factors c-rel and RelA Control Epidermal Development and Homeostasis in Embryonic and Adult Skin via Distinct Mechanisms

Raffi Gugasyan,[1] Anne Voss,[1] George Varigos,[2] Tim Thomas,[1] Raelene J. Grumont,[1] Pritinder Kaur,[3] George Grigoriadis,[1] and Steve Gerondakis[1]*

*The Walter and Eliza Hall Institute of Medical Research[1] and Royal Melbourne Hospital,[2] Parkville, Victoria 3050, and Peter MacCallum Cancer Institute, East Melbourne, Victoria 3002,[3] Australia*

Received 11 January 2004 /Returned for modification 25 February 2004 /Accepted 19 April 2004

**Determining the roles of Rel/NF-κB transcription factors in mouse skin development with loss-of-function mutants has been limited by redundancy among these proteins and by embryonic lethality associated with the absence of RelA. Using mice lacking RelA and c-rel, which survive throughout embryogenesis on a tumor necrosis factor alpha (TNF-α)-deficient background (*rela*$^{-/-}$ c-*rel*$^{-/-}$ *tnf*α$^{-/-}$), we show that c-rel and RelA are required for normal epidermal development. Although mutant fetuses fail to form tylotrich hair and have a thinner epidermis, mutant keratinocyte progenitors undergo terminal differentiation to form an outer cornified layer. Mutant basal keratinocytes are abnormally small, exhibit a delay in $G_1$ progression, and fail to form keratinocyte colonies in culture. In contrast to the reduced proliferation of mutant keratinocytes during embryogenesis, skin grafting experiments revealed that the mutant epidermis develops a TNF-α-dependent hyperproliferative condition. Collectively, our findings indicate that RelA and c-rel control the development of the epidermis and associated appendages during embryogenesis and regulate epidermal homeostasis in a postnatal environment through the suppression of innate immune-mediated inflammation.**

The epidermis is a stratified epithelium consisting of proliferating and differentiating keratinocytes that generates an external barrier. The epidermis comprises four major layers. The innermost basal layer contains the quiescent long-lived stem cell population and rapidly dividing transit-amplifying (TA) cells, the progeny of stem cells (61). TA cells normally undergo a limited number of divisions before withdrawing from the cell cycle to commence differentiation while migrating through the suprabasal layers of the epidermis (stratum spinosum and stratum granulosum) to produce the outer epidermal layer, the stratum corneum. Keratinocytes in the stratum corneum are terminally differentiated, enucleated cells that combine with the cornified envelope to generate an impermeable outer barrier. Coupled with the ongoing homeostatic maintenance of the epidermis, the skin must respond to stress arising from a wide variety of insults, which in the case of microbial invasion involves activating and recruiting the innate immune system. Abnormalities in the response to these insults can lead to pathologies associated with immune-mediated inflammatory skin disease and cutaneous neoplasms.

Among the intracellular signaling pathways implicated in the development of skin is the Rel/NF-κB pathway. The transcriptional mediators of this pathway comprise dimers of related subunits (c-rel, RelA, RelB, NF-κB1, and NF-κB2). c-rel, RelA, and RelB possess C-terminal transcriptional transactivation domains. NF-κB1 (p50) and NF-κB2 (p52) lack intrinsic transactivating properties and function as homodimeric transcriptional repressors or modulators of transactivating dimer partners (3). In most cells, the majority of Rel/NF-κB proteins are retained in a latent cytoplasmic state through association with inhibitory (IκB) proteins (63). Numerous stimuli activate an IKK kinase complex (α, β, and γ subunits) in which IKKβ phosphorylates IκB proteins (29), targeting them for ubiquitin-dependent proteosome-mediated degradation. Rel/NF-κB dimers then translocate to the nucleus, where they control transcription by binding to decameric sequences (κB elements) found within the transcriptional regulatory regions of target genes (14). An alternative Rel/NF-κB activation pathway has also been identified in which the NF-κB2 precursor p100 is processed to a mature form (p52NF-κB2) in an IKKα-dependent manner (53).

Skin defects are present in a number of mouse models in which Rel/NF-κB function is perturbed. The various skin phenotypes observed in these models, which in some instances appear contradictory, serve to emphasize the multitude of roles that the Rel/NF-κB pathway is likely to play in the skin. Mice lacking IKKα have a thickened stratum spinosum and lack the granular and corneal layers (23, 37, 56), a phenotype consistent with the impaired capacity of these keratinocytes to proliferate and differentiate in culture (24). Recent studies indicate that the skin defects observed in *ikk*α$^{-/-}$ mice appear to be Rel/NF-κB independent (24). The embryonic death of *ikk*β$^{-/-}$ mice at embryonic day ≈13 (E13) from fetal hepatocyte apoptosis (38, 57) has to date precluded an investigation of IKKβ function throughout the skin. However, conditional elimination of IKKβ within basal keratinocytes does not disrupt embryonic epidermal differentiation, instead triggering a severe inflammatory skin condition following birth (44).

Loss of IKKγ in mice resembles the human X-linked disorder incontinentia pigmenti. Unlike *ikk*γ$^{-/-}$ male mice, which

* Corresponding author. Mailing address: The Walter and Eliza Hall Institute of Medical Research, 1G Royal Parade, Parkville, Victoria 3050, Australia. Phone: 61393452542. Fax: 61393470852. E-mail: gerondakis@wehi.edu.au.

die at ≈E12 from hepatocyte apoptosis, *ikkγ*$^{+/-}$ females survive and display skin defects characterized by epidermal hyperproliferation, hyperkeratosis, hyperpigmentation, and inflammation (39, 47, 49). A range of phenotypes were also observed in transgenic mice expressing a nondegradable mutant form of IκB-α within the skin, which acts as a constitutive repressor of NF-κB signaling. Keratin-14 promoter-targeted expression of mutant IκB-α led to a hyperproliferative skin condition (52, 60). Constitutive ubiquitous expression of an IκB-α transgene did not lead to epidermal basal cell hyperproliferation, instead causing defects in hair follicle and exocrine gland development (50). Conversely, sustained NF-κB activity in *Iκbα*$^{-/-}$ mice resulted in a severe dermatitis that appears to be mediated by hematopoietic cells (5, 32).

In contrast to the skin defects displayed by mice lacking different IKK subunits, viable mutants lacking c-rel, NF-κB1, or NF-κB2 exhibit no skin defects. Rather, the essential functions of these individual transcription factors are restricted to the immune system (12). Although loss of RelA results in embryonic lethality at ≈E14.5 due to tumor necrosis factor alpha (TNF-α)-mediated fetal hepatocyte apoptosis (6), skin defects have not been reported in viable *rela*$^{-/-}$ *tnfα*$^{-/-}$ and *rela*$^{-/-}$ *tnfr1*$^{-/-}$ mutants (1, 9, 46). The exception among the individual Rel/NF-κB null mutants is *relb*$^{-/-}$ mice, which develop a T-cell-dependent inflammatory dermatitis (4).

The findings arising from the IKK null mutants and IκB-α transgenic mice indicated that the absence of a skin phenotype in the single Rel/NF-κB mutant mice was largely due to redundancy among these transcription factors. Given that viable mice lacking two Rel/NF-κB members such as the *nf*κb1$^{-/-}$ c-*rel*$^{-/-}$ (45) and *nf*κb1$^{-/-}$ *nf*κb2$^{-/-}$ (10, 26) mutants did not exhibit skin defects, this suggested that RelA in combination with other family members may be important in skin development and function. To address this issue, we generated RelA/NF-κB1 and RelA/c-rel compound null mutant mice on a TNF-α-deficient background as a means of bypassing the embryonic lethality associated with loss of RelA function. While TNF-α is an important mediator of inflammatory responses and is required for the normal architecture of lymphoid organs (51), the absence of skin defects in *tnfα*$^{-/-}$ and *tnfr1*$^{-/-}$ mice indicates that this cytokine is dispensable for epidermal development.

The *nf*κb1$^{-/-}$ *rela*$^{-/-}$ *tnfα*$^{-/-}$ mutants did not display an overt phenotype in the skin, whereas fetal mice lacking RelA and c-rel displayed multiple epidermal defects, a finding consistent with the pattern of c-*rel* expression in the epidermis during development. Coupled with the onset of innate immune-mediated epidermal inflammation in grafted *rela*$^{-/-}$ c-*rel*$^{-/-}$ *tnfα*$^{-/-}$ skin, our findings indicate that c-rel and RelA are key transcriptional regulators of skin development and homeostasis.

## MATERIALS AND METHODS

**Mice.** *rela*$^{-/-}$ c-*rel*$^{-/-}$ *tnfα*$^{-/-}$ and *rela*$^{-/-}$ *nf*κb1$^{-/-}$ *tnfα*$^{-/-}$ mutants were produced by intercrossing *rela*$^{+/-}$ c-*rel*$^{-/-}$ *tnfα*$^{-/-}$ and *rela*$^{+/-}$ *nf*κb1$^{-/-}$ *tnfα*$^{-/-}$ mice, respectively. Due to early neonatal lethality of *rela*$^{-/-}$ c-*rel*$^{-/-}$ *tnfα*$^{-/-}$ and *rela*$^{-/-}$ *nf*κb1$^{-/-}$ *tnfα*$^{-/-}$ mice, timed matings were established where day 0 was defined upon observation of a vaginal plug.

**Histology.** For paraffin sections, embryos or fetal dorsal skin was fixed in 4% paraformaldehyde, cut at a thickness of 5 μm, and mounted onto 3-aminopropyltriethoxy-silane (AES)-coated slides. For frozen sections, dorsal skin was embedded in OCT (Tissue-Tek), snap-frozen on dry ice, and sectioned at a thickness of 5 μm. The tissues were mounted onto AES-coated slides and fixed in acetone. Epidermal thickness was measured in 400× images (NIH Image 1.63 f) of *rela*$^{-/-}$ c-*rel*$^{-/-}$ *tnfα*$^{-/-}$ mutants versus *rela*$^{+/+}$ c-*rel*$^{-/-}$ *tnfα*$^{-/-}$ controls. The two largest and the two smallest thicknesses per view field were measured to account for the folding of the epidermis. Two-factor analysis of variance with Scheffe's post hoc test was used to analyze the data with genotype and crest versus crease of the epidermal fold as the two factors. The hair follicles were counted along 870 μm of epidermis. The data were compared by Student's *t* test. Results are given as means ± standard errors of the means.

**Immunohistochemistry.** Paraffin tissue sections were deparaffinized and rehydrated through a graded ethanol series. The sections were blocked with a 1% bovine serum albumin–10% normal goat serum (NGS)–0.2% Triton X-100 solution. Primary antibodies used were a mouse anti-human PCNA monoclonal antibody (clone PC10 immunoglobulin G2a; Pharmingen) and rabbit anti-keratin-6 antibody (gift of Joe Rothnagel). A goat anti-mouse immunoglobulin secondary antibody was used to bind the anti-PCNA antibody (Santa Cruz), and all rabbit polyclonal antibodies were detected with the universal horse anti-rabbit immunoglobulin secondary antibody (Vector Labs). Tissues were then stained with the ABC peroxidase kit (Vector Labs) and counterstained with hematoxylin and eosin (H&E).

**Immunofluorescence.** For indirect immunofluorescence, frozen sections were treated with a blocking solution (2% gelatin, 1% Triton X-100, 5% fetal bovine serum, and 5% NGS in phosphate-buffered saline). Three incubation steps were conducted to achieve double staining of tissue sections. The rabbit anti-mouse antibodies used for the primary incubation were to keratin-14, keratin-10, loricrin, filaggrin (Babco), and involucrin (a gift of S. Ting). Tissues were incubated with an Alexa-goat anti-rabbit secondary antibody (Molecular Probes), while the third incubation was with fluorescein isothiocyanate-labeled polyclonal antibodies to loricrin (Babco) or keratin-10 (Babco).

**In vivo bromodeoxyuridine labeling and tissue staining.** Pregnant mothers injected intraperitoneally with bromodeoxyuridine (100 μg/g; Sigma) were sacrificed 1 h later, and E18 fetuses were removed. Paraffin skin sections were stained with the antibromodeoxyuridine antibody (Bio-Science Products) for 1 h. The sections were incubated for a further hour with the universal horse anti-mouse biotinylated secondary antibody (Vector Labs).

**In situ hybridization.** A probe encoding part of the mouse c-*rel* cDNA (nucleotides 403 to 1621; GenBank accession no. X15842) was cloned into pBKS. To produce a radiolabeled antisense riboprobe, this plasmid was linearized with HindIII and transcribed with T7 RNA polymerase in the presence of $^{33}$P-labeled UTP (Amersham). In situ hybridization was performed essentially as described before (59).

**TUNEL staining.** Terminal deoxynucleotidyltransferase-mediated dUTP-biotin nick end labeling (TUNEL) staining of paraffin-embedded skin sections was performed according to the manufacturer's instructions (ApopTag TUNEL staining kit; Serologicals Corporation).

**Isolation of basal keratinocytes.** Skin flanks excised from E18 fetuses were incubated overnight at 4°C in Dispase II (2 mg/ml). The epidermis was separated from the dermis and briefly treated with trypsin to release basal keratinocytes. The reaction was terminated by the addition of soybean inhibitor, and cell viability was determined by trypan blue exclusion.

**Cell culture and stains.** Isolated basal keratinocytes were seeded at a density of $10^6$ cells in a six-well plate (Costar) in serum-free keratinocyte medium (Gibco-BRL) supplemented with hydrocortisone (0.5 μg/ml) and low levels of $CaCl_2$ (0.02 mM). Cultures were fixed in 2% formaldehyde and subjected to immunoperoxidase staining for keratin-14 (LL001, immunoglobulin G2a; a gift of Irene Leigh). Cells were then incubated with biotinylated secondary antibodies (Vector Laboratories), followed by streptavidin-horseradish peroxidase (ABC kit; Vector Laboratories) and enzyme substrate (AEC substrate kit; Vector Laboratories).

**Flow cytometry and cell cycle analysis.** Basal keratinocytes were stained with fluorescein isothiocyanate-conjugated rat anti-human integrin-α6 antibody (BD Pharmingen) and phycoerythrin-conjugated anti-mouse CD71 antibody (BD Pharmingen) in a two-color reaction or stained with a fluorescein isothiocyanate-conjugated anti-mouse CD29 antibody (integrin-β1) (Cymbus Biotechnology) in a single-color reaction. Stained keratinocytes were either cell sorted or analyzed immediately with a FACScan. Propidium iodide (20 μg/ml) was added to exclude dead cells during the analysis. For cell cycle analysis on a FACScan, TA cells (integrin-α6$^{hi}$ CD71$^{hi}$) were fixed with chilled 70% ethanol and treated with propidium iodide and RNase. Cell cycle profiles were analyzed with the Modfit software program.

**Skin grafts.** *B6rag-1*$^{-/-}$ or *B6rag-1*$^{-/-}$ *tnfα*$^{-/-}$ mice (11 to 15 weeks of age) were anaesthetized with Penthrane, and the graft bed was prepared by removing a 1.5-cm$^2$ area of skin above the ribcage. A 1-cm$^2$ area of dorsal skin excised from

an E18 fetus was placed into the graft bed and dressed with Jelonet gauze (Smith & Nephew) and 3M micropore surgical tape. Bandages were routinely removed after 8 days.

**Skin permeability assay.** Epidermal barrier function was determined as previously described (20).

**Northern and Western blotting.** We subjected 5-μg samples of total RNA isolated from purified basal keratinocytes to Northern blotting essentially as described before (17). Filters were sequentially probed with a 1.4-kb XhoI mouse c-*myc* cDNA, a rat 1.1-kb PstI glyceraldehhyde-3-phosphate dehydrogenase cDNA, and a 0.4-kb BamHI mouse keratin-14 cDNA (gift of J. Rothnagel). Protein blots were performed essentially as described before (43) with equivalent amounts of total cellular protein isolated from purified control and mutant keratinocytes. Filters were probed with either mouse anti-cyclin D1 monoclonal immunoglobulin (Santa Cruz Biotechnology), rabbit anti-cyclin D2 polyclonal immunoglobulin (Santa Cruz Biotechnology), or rat anti-HSP70 monoclonal antibody (gift of D. Huang).

**Cell size measurements.** Each of four control (*rela*$^{+/+}$ c-*rel*$^{-/-}$ *tnf*α$^{-/-}$) and mutant (*rela*$^{-/-}$ c-*rel*$^{-/-}$ *tnf*α$^{-/-}$) fetuses were used for epidermal basal keratinocyte size measurements. To avoid stretching and contraction artifacts, skin overlying the nuchal fat pad attached to the body of E18.5 and E19.5 pups was analyzed. Images of control and mutant skin were taken at 1,000× magnification with a compound microscope and a digital camera (Zeiss). Images were analyzed with an image analysis program (NIH Image 1.63f). The areas of all basal cell profiles were measured per image. Seven to nine images representing 85 to 112 basal cells were analyzed per animal. Results are given as the mean ± standard error of the mean. Data were analyzed statistically with a two-factor analysis of variance with the genotype and the developmental age as the factors and Scheffe's method for pairwise comparison with StatView 4.5 software.

## RESULTS

**Disrupting the TNF signaling pathway rescues embryonic death resulting from a combined absence of NF-κB1 and RelA or c-rel and RelA.** In order to examine what overlapping roles NF-κB1 and RelA or c-rel and RelA might serve during skin development, these compound Rel/NF-κB mutants were generated on a TNF-α-deficient background to overcome the death at ≈E13.5. The birth of *nf*κb1$^{-/-}$ *rela*$^{-/-}$ *tnf*α$^{-/-}$ and *rela*$^{-/-}$ c-*rel*$^{-/-}$ *tnf*α$^{-/-}$ mice from the respective *rela*$^{+/-}$ c-*rel*$^{-/-}$ *tnf*α$^{-/-}$ or *nf*κb1$^{-/-}$ *rela*$^{+/-}$ *tnf*α$^{-/-}$ intercrosses established that if TNF-α-mediated hepatocyte apoptosis was prevented, the absence of NF-κB1 or c-rel in combination with a lack of RelA did not prevent murine embryogenesis from proceeding beyond E13.5.

While *rela*$^{-/-}$ c-*rel*$^{-/-}$ *tnf*α$^{-/-}$ mice were born at a frequency of ≈25%, the number of newborn *nf*κb1$^{-/-}$ *rela*$^{-/-}$ *tnf*α$^{-/-}$ mice was lower than expected, suggesting that some embryonic death at a developmental stage yet to be determined occurred in the absence of NF-κB1 and RelA. The gross morphology of E18 (Fig. 1A) and newborn *rela*$^{-/-}$ c-*rel*$^{-/-}$ *tnf*α$^{-/-}$ and *nf*κb1$^{-/-}$ *rela*$^{-/-}$ *tnf*α$^{-/-}$ mice appeared relatively normal. The most notable difference was a reduced body weight of ≈30% for *rela*$^{-/-}$ c-*rel*$^{-/-}$ *tnf*α$^{-/-}$ E18 fetuses and newborn mice compared with littermate controls (results not shown). Despite the relatively normal appearance of *rela*$^{-/-}$ c-*rel*$^{-/-}$ *tnf*α$^{-/-}$ and *nf*κb1$^{-/-}$ *rela*$^{-/-}$ *tnf*α$^{-/-}$ newborns, both mutant types died within 12 h of birth from as yet unknown causes.

Concerns that stress associated with the neonatal death of these mutants might indirectly affect skin architecture prompted us to perform all subsequent studies on fetal skin. We chose to focus on dorsal skin, as it represents a location in which epidermal and hair follicle morphogenesis is well advanced in a fetus. Microscopic examination of stained histological sections revealed that at E18, control fetuses (wild type, *tnf*α$^{-/-}$, c-*rel*$^{-/-}$, *nf*κb1$^{-/-}$, *nf*κb1$^{-/-}$ *tnf*α$^{-/-}$, c-*rel*$^{-/-}$ *tnf*α$^{-/-}$ and *rela*$^{-/-}$ *tnf*α$^{-/-}$, of which the c-*rel*$^{-/-}$ *tnf*α$^{-/-}$ skin shown in Fig. 1B is a typical example) displayed a well-defined epidermis with numerous hair follicles at different stages of differentiation. Although *nf*κb1$^{-/-}$ *rela*$^{-/-}$ *tnf*α$^{-/-}$ embryonic skin (Fig. 1C) was similar in appearance to that of controls, a marginal reduction in epidermal thickness was consistently noted. In contrast, the *rela*$^{-/-}$ c-*rel*$^{-/-}$ *tnf*α$^{-/-}$ epidermis was distinctly thinner, and the hair follicles comprised only a few rudimentary buds (Fig. 1D). As the skin defects were most profound in the combined absence of RelA and c-rel, all subsequent analysis focused on the *rela*$^{-/-}$ c-*rel*$^{-/-}$ *tnf*α$^{-/-}$ mice.

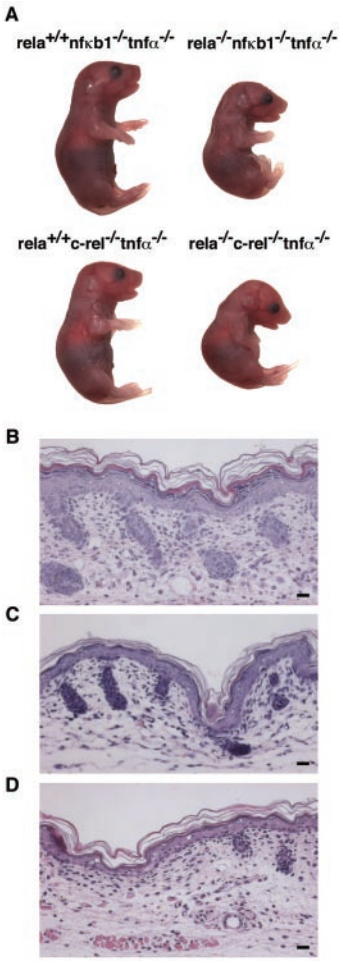


FIG. 1. Embryonic death resulting from the combined loss of NF-κB1 and RelA or c-rel and RelA is overcome by blocking TNF-α signaling. (A) *rela*$^{-/-}$ *nf*κb1$^{-/-}$ *tnf*α$^{-/-}$ or *rela*$^{-/-}$ c-*rel*$^{-/-}$ *tnf*α$^{-/-}$ fetuses were isolated at E18 from the respective intercrosses of *rela*$^{+/-}$ *nf*κb1$^{-/-}$ *tnf*α$^{-/-}$ and *rela*$^{+/-}$ c-*rel*$^{-/-}$ *tnf*α$^{-/-}$ mice. (B to D) H&E-stained sections of dorsal skin from E18 fetuses. (B) *rela*$^{+/+}$ c-*rel*$^{-/-}$ *tnf*α$^{-/-}$, (C) *rela*$^{-/-}$*nf*κb1$^{-/-}$ *tnf*α$^{-/-}$, and (D) *rela*$^{-/-}$ c-*rel*$^{-/-}$ *tnf*α$^{-/-}$ genotypes. Bar, 425 μm.

**c-rel is expressed in the epidermis and in hair follicles.** Epidermal and hair follicle defects in the combined absence of RelA and c-rel indicated that both transcription factors probably shared overlapping patterns of expression within the skin. While a role for RelA in the epidermis was consistent with its ubiquitous expression (56), c-rel function was thought to be

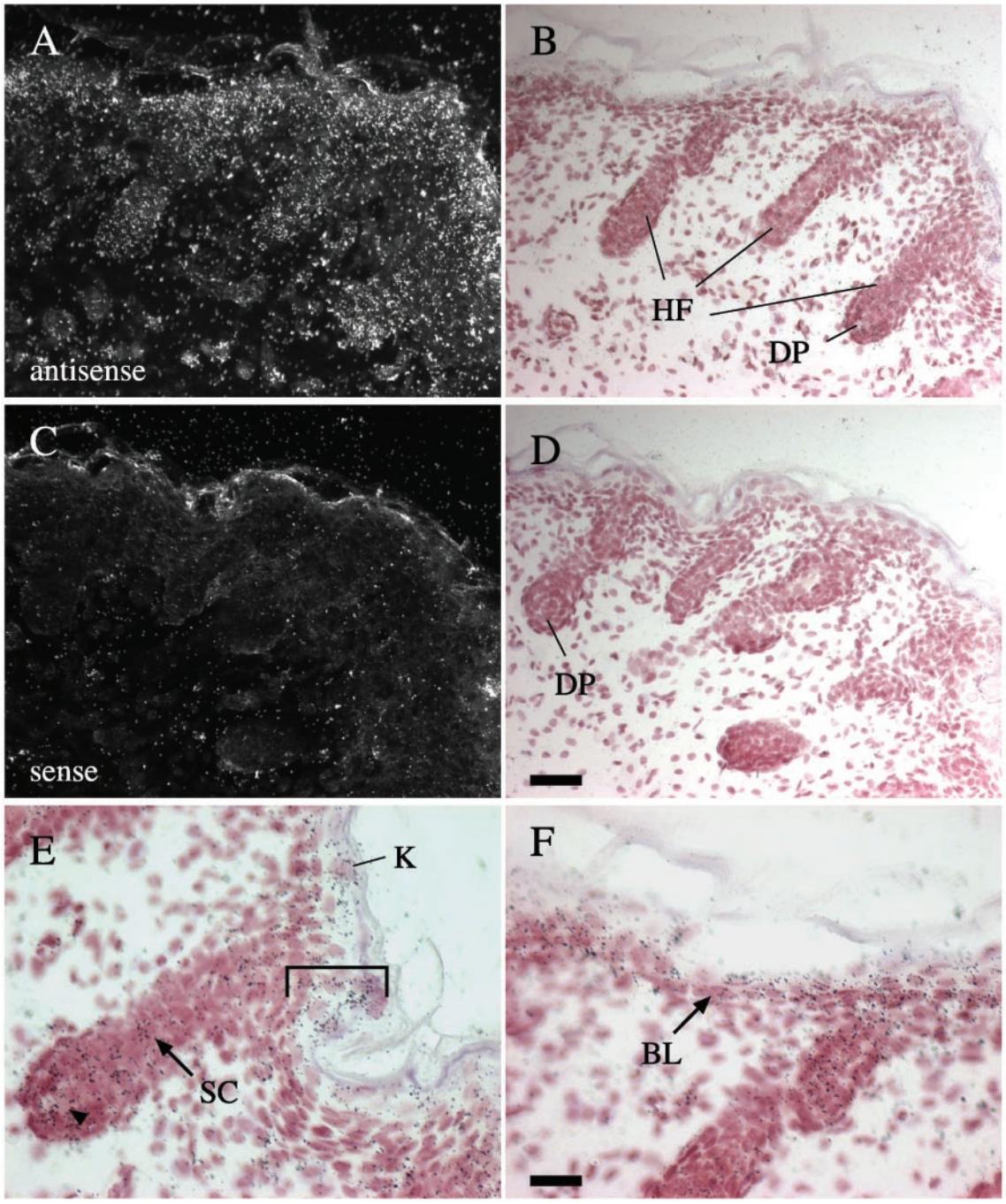


FIG. 2. c-*rel* mRNA is expressed in fetal skin. A c-*rel* cRNA probe was incubated with sections of E18.5 skin. Panels A and C are dark-field images of the corresponding bright-field images in panels B and D. Sense probe controls are shown in panels C and D. Note the c-*rel* mRNA expression in the epidermis and hair follicles (A). At higher magnification (E and F), silver grains overlay the sheath cells (arrow in panel E) and the dermal papilla (arrowhead in panel E) of hair follicles, plus basal cells (arrow in panel F) and differentiating keratinocytes in the epidermis (bracket in panel E). HF, hair follicle; SC, sheath cells; DP, dermal papilla; BL, basal layer; K, keratinocytes. Bars: 43 μm (A, B, C, and D) and 22 μm (E and F).

hematopoiesis restricted (33). To assess the relationship between the skin defects observed in the *rela*$^{-/-}$ c-*rel*$^{-/-}$ *tnf*$\alpha^{-/-}$ mice and c-*rel* expression in the skin, in situ hybridization was performed on sagittal sections of C57BL/6 embryos at E15.5 and back skin sections from a C57BL/6 E18.5 fetus. In E15.5 embryos, no c-*rel* expression above background could be detected in the skin (results not shown). At E18.5, low-level expression of c-*rel* mRNA was detected in the epidermis and in hair follicles (Fig. 2A and B). In the epidermis, c-*rel* mRNA was present in basal cells as well as in the spinous and granular layers (Fig. 2E and F). Differentiating keratinocytes appeared to maintain c-*rel* expression while these cells contained a nu-

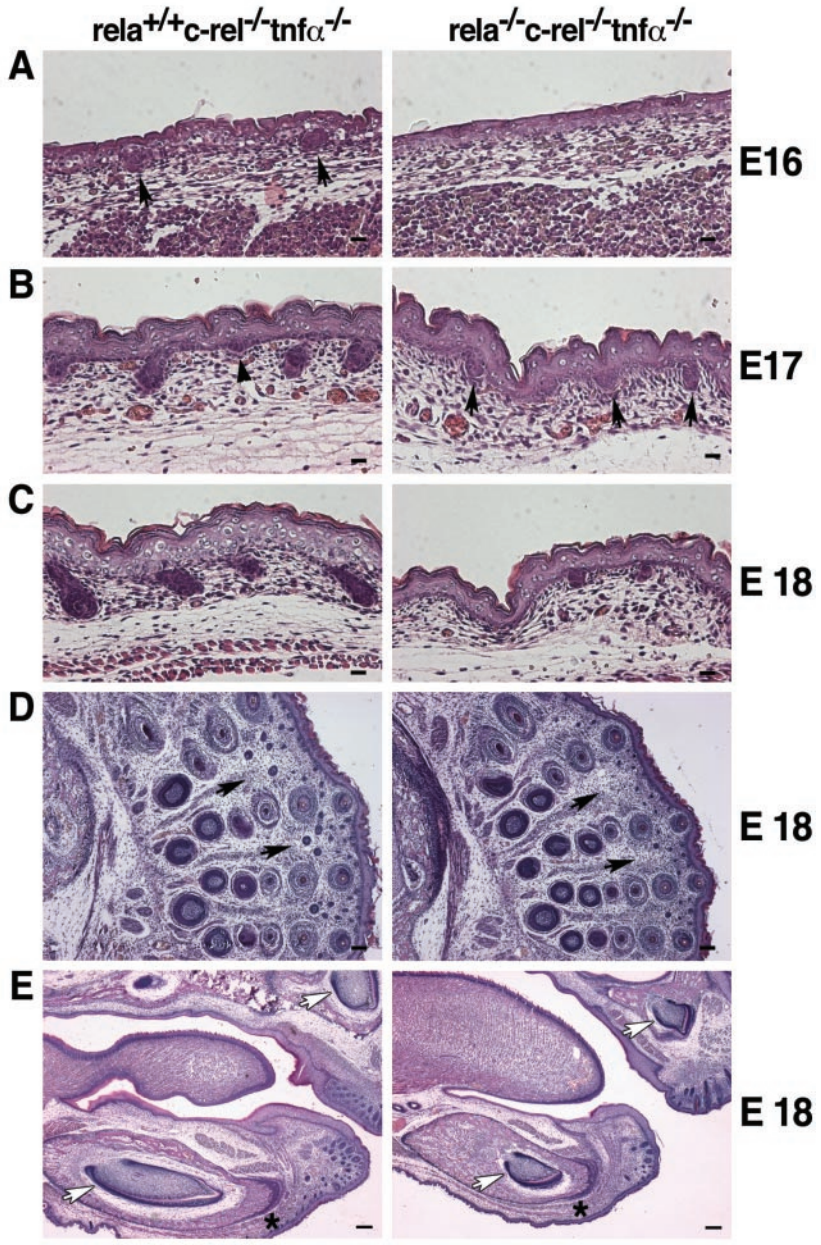


FIG. 3. Hair follicle morphogenesis and tooth development are impaired in the absence of c-rel and RelA. (A to C) Hair follicle development in control (*rela*$^{+/+}$ c-*rel*$^{-/-}$ *tnf*$\alpha^{-/-}$) and mutant (*rela*$^{-/-}$ c-*rel*$^{-/-}$ *tnf*$\alpha^{-/-}$) fetal sections stained with H&E. Bar, 425 μm. (A) E16. Hair placodes (tylotrich) are evident in control (black arrows) but not mutant skin. (B) E17. In controls, continuing development of tylotrich hair follicles is evident, along with a new wave (awl type, arrowhead) of hair placodes that are also evident in mutant skin (awl type; arrow). (C) E18. In control skin, tylotrich and awl hair follicles have developed further. Only premature buds are evident in the mutant skin. (D and E) Serial sections of E18 control and mutant embryos stained with H&E. (D) Mystacial vibrissa follicles develop normally in mutant embryos Bar, 1,600 μm. Note the paucity of hair follicles (arrow) between the whiskers. (E) The outgrowth of incisor teeth (arrow) was impaired in the mutant embryo. Note the lack of hair follicles (asterisks) adjacent to the vibrissa follicles. Bar, 875 μm.

cleus, suggesting that its expression continued until the terminal stage of keratinocyte differentiation. In hair follicles, c-*rel* was expressed in the sheath cells, the hair bulb, and the dermal papilla (Fig. 2E). c-*rel* was also expressed in a few scattered cells within the dermis (Fig. 2E). These findings confirm that c-*rel* is normally expressed in those skin structures that develop abnormally in *rela*$^{-/-}$ c-*rel*$^{-/-}$ *tnf*$\alpha^{-/-}$ mice.

**Impaired hair follicle morphogenesis in *rela*$^{-/-}$ c-*rel*$^{-/-}$ *tnf*$\alpha^{-/-}$ mice.** Mice have four hair types (tylotrich, awl, auchene, and zigzag) (40). During embryogenesis, two distinct waves of hair follicle morphogenesis occur. The first wave (tylotrich or guard hair) commences around E14. By E17, a second wave of hair placodes appears, coinciding with the initiation of awl hair development. To determine at which

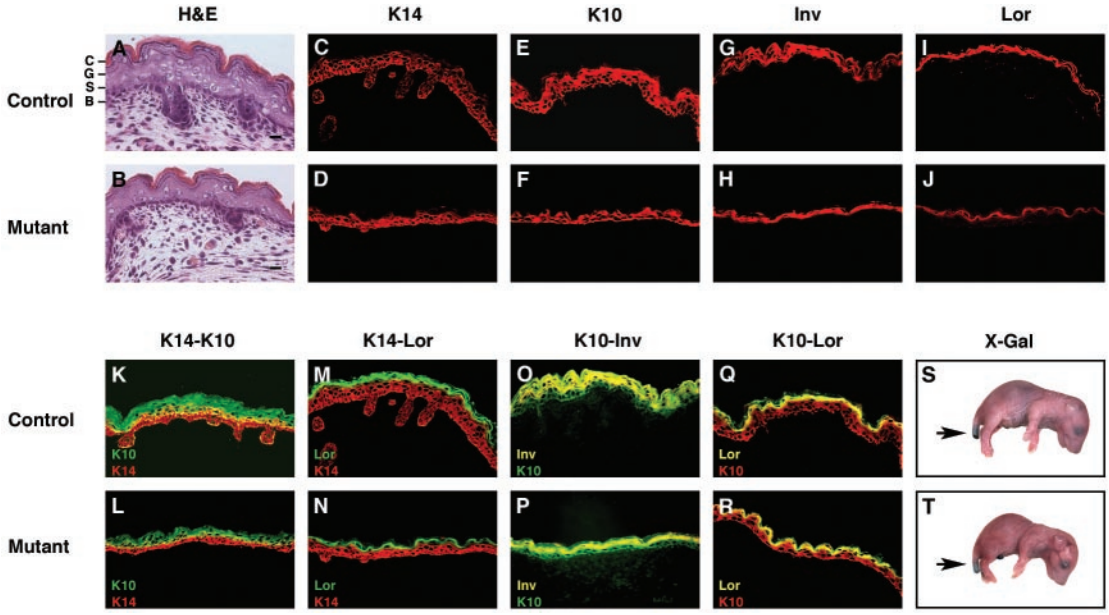


FIG. 4. Epidermal differentiation is impaired in *rela*$^{-/-}$ c-*rel*$^{-/-}$ *tnfα*$^{-/-}$ embryos. Biochemical markers were used to analyze keratinocyte differentiation in control ($n = 5$; *rela*$^{+/+}$ c-*rel*$^{-/-}$ *tnfα*$^{-/-}$) and mutant ($n = 5$; *rela*$^{-/-}$ c-*rel*$^{-/-}$ *tnfα*$^{-/-}$) E18 dorsal skin. H&E-stained sections of (A) control and (B) mutant dorsal skin depict the basal layer (B), the stratum spinosum (S), the stratum granulosum (G), and stratum corneum (C). Bar, 225 μm. Frozen sections of control (C, E, G, and I) and mutant (D, F, H, and J) dorsal skin were subjected to indirect immunofluorescent staining for keratin-14 (K14), keratin-10 (K10), involucrin (Inv), and loricrin (Lor) expression. Two-color immunofluorescent staining was performed on control (K, M, O, and Q) and mutant (L, N, P, and R) dorsal skin. Stains are representative of five experiments (yellow represents colocalization of Alexa and fluorescein isothiocyanate fluorochromes). (S and T) X-Gal staining of E18 fetuses was performed to assess epidermal barrier function. Except where the tail was excised (arrow), the dye did not penetrate control or mutant fetuses.

point during embryogenesis follicle development is impaired in the absence of RelA and c-rel, histological sections of E16, -17, and -18 control and mutant embryos were examined.

In control embryos (*rela*$^{+/+}$ c-*rel*$^{-/-}$ *tnfα*$^{-/-}$), hair placodes were present in E16 dorsal skin, consistent with the first wave of placode development having been initiated (Fig. 3A). At E17, new hair placodes were present, and follicles associated with the first wave of hair development had begun to develop hair shaft cells (Fig. 3B). By E18, the development of both groups of follicles had progressed further (Fig. 3C). By contrast, mutant skin (*rela*$^{-/-}$ c-*rel*$^{-/-}$ *tnfα*$^{-/-}$) showed no evidence of placode formation at E16 (Fig. 3A). However, by E17, the first hair placodes were observed in mutant fetuses, albeit in markedly reduced numbers (Fig. 3B). In the skin of E18 mutant mice, only a few premature follicles were present, and these had failed to develop hair shafts (Fig. 3C). The number of hair follicles was reduced by 70% in *rela*$^{-/-}$ c-*rel*$^{-/-}$ *tnfα*$^{-/-}$ mutants compared to *rela*$^{+/+}$ c-*rel*$^{-/-}$ *tnfα*$^{-/-}$ controls (4.3 ± 0.9 hair follicles along an 870-μm stretch of epidermis versus 14.4 ± 0.4; $P < 0.0001$; $n = 4$ and 5 embryos, respectively). Whiskers were also examined in serial sections of control and mutant fetuses. No obvious defects were observed in the maturation or number of developing mystacial and supernumerary vibrissa follicles of *rela*$^{-/-}$ c-*rel*$^{-/-}$ *tnfα*$^{-/-}$ fetuses (Fig. 3D), indicating that c-rel and RelA are dispensable for whisker development.

Interestingly, an examination of the embryonic teeth, which are epidermal appendages, revealed that the molars and incisors were abnormally small in the *rela*$^{-/-}$ c-*rel*$^{-/-}$ *tnfα*$^{-/-}$ fetuses (Fig. 3E and data not shown). As the developmental status of the surrounding structures appeared normal for an E18 fetus, the smaller teeth in the mutants were unlikely to reflect a delay in development. Collectively, these findings indicate that RelA and c-rel are required for the normal development of certain hair types and epithelial appendages, such as teeth.

**Abnormal epidermal development in the combined absence of RelA and c-rel.** We next focused on epidermal development in *rela*$^{-/-}$ c-*rel*$^{-/-}$ *tnfα*$^{-/-}$ mice. A comparison of H&E-stained sections from E18 control and mutant mice revealed that the basal, spinous, granular, and cornified layers of the skin were present in fetuses of both genotypes (Fig. 4A and B). However, the mutant epidermis was noticeably thinner, with fewer differentiating keratinocytes in the suprabasal region compared with age-matched controls (Fig. 3C and 4A and B). The epidermal thickness was reduced by 36% in *rela*$^{-/-}$ c-*rel*$^{-/-}$ *tnfα*$^{-/-}$ mutants compared to *rela*$^{+/+}$ c-*rel*$^{-/-}$ *tnfα*$^{-/-}$ controls (30.8 ± 2.2 versus 48.2 ± 3.6 μm; $P < 0.0001$; $n = 5$ and 3 embryos, respectively). The cells in the basal layer of *rela*$^{-/-}$ c-*rel*$^{-/-}$ *tnfα*$^{-/-}$ skin were organized differently from those of controls, and the basal cell profiles appeared smaller in stained sections of *rela*$^{-/-}$ c-*rel*$^{-/-}$ *tnfα*$^{-/-}$ fetuses (Fig. 4A and B). Measurement of basal cell size in *rela*$^{-/-}$ c-*rel*$^{-/-}$ *tnfα*$^{-/-}$ and *rela*$^{+/+}$ c-*rel*$^{-/-}$ *tnfα*$^{-/-}$ mice confirmed that the mean basal cell profile area was reduced by ≈33% (0.397 ± 0.014 versus 0.592 ± 0.019 μm; $P < 0.0001$) in the *rela*$^{-/-}$ c-*rel*$^{-/-}$ *tnfα*$^{-/-}$ mutant. The age of the fetus (E18.5 or E19.5) did not significantly influence the cell profile size ($P = 0.67$).

To determine if keratinocyte differentiation was impaired in the absence of c-rel and RelA, we examined the expression of proteins that characterize specific epidermal layers. Keratin-14

protein is normally expressed in basal cells and hair follicles (11). Although anti-keratin-14 antibodies stained the innermost basal cells at the dermal-epidermal boundary of both control and mutant skin (Fig. 4C and D), the staining that was usually two cell layers thick in the control was generally confined to one cell layer in the mutant, with little spinous staining. The early differentiation marker keratin-10 is expressed predominantly in the suprabasal spinous and granular layers (11). In the control epidermis, anti-keratin-10 antibody staining of the suprabasal layers was at least three cell layers thick. In the mutant epidermis, keratin-10 expression was confined to two cell layers (Fig. 4E and F). The late differentiation markers involucrin and loricrin are major components of the cornified envelope, with involucrin expressed in the upper spinous and granular layers, while loricrin is restricted to the granular layer (28, 36). Involucrin and loricrin staining was confined to these layers in the mutant epidermis, the region in which these proteins were expressed being somewhat compacted compared with control skin (Fig. 4G, H, I, and J).

The stratification of the mutant skin was next examined with double immunofluorescence staining. In control epidermis, costaining with antibodies to keratin-14 and keratin-10 revealed a significant region of colocalization (shown in yellow), indicative of keratinocytes leaving the basal layer and entering the spinous layer (Fig. 4K). Colocalization of keratin-14 and keratin-10 was reduced in the mutant epidermis (Fig. 4L). Staining for keratin-14 and loricrin revealed that basal and spinosal expression of these proteins in the granular layer was distinct in both control and mutant epidermis (Fig. 4M and N). While costaining for keratin-10 and involucrin revealed the expected pattern of overlapping expression in the upper spinous and granular layers, the region of coexpression was markedly reduced in mutant fetuses compared with controls (Fig. 4O and P). The region of keratin-10 and loricrin coexpression was only marginally reduced in the mutant epidermis (Fig. 4Q and R), and the expression levels of filaggrin, a marker for terminally differentiated enucleated squames, were equivalent in control and mutant epidermis (not shown). Taken together, these data show that the suprabasal layers were reduced in *rela*$^{-/-}$ c-*rel*$^{-/-}$ *tnf*$\alpha^{-/-}$ fetal skin.

To determine if the differences in the mutant epidermis resulted in barrier dysfunction, dye penetration assays were performed by immersing control and mutant E18 fetuses overnight in an 5-bromo-4-chloro-3-indolyl-β-D-galactopyranoside (X-Gal) solution. These experiments demonstrated that dye did not penetrate the skin of either control or mutant fetuses (Fig. 4S and T), except at the site of the tail biopsy wound. Hence barrier function of the mutant epidermis is intact. Collectively, these findings establish that in the combined absence of c-rel and RelA, epidermal development is abnormal, but keratinocytes still appear able to undergo terminal differentiation.

**Epidermal stem cell and transit-amplifying cell numbers are normal in the absence of c-rel and RelA.** Cell surface marker expression has been used to delineate the stem cell, TA cell, and maturing keratinocyte populations in the epidermis (62). Stem cells and TA cells both express integrin β1, with the highest levels expressed by stem cells (27). Integrin α6 expression is high in stem cells and TA cells, whereas keratinocytes committed to differentiation express low levels of this integrin (35). Transferrin receptor (CD71) expression has also been used to distinguish between quiescent stem cells (integrin α6$^{hi}$ CD71$^{lo}$) and proliferating TA cells (integrin α6$^{hi}$ CD71$^{hi}$).

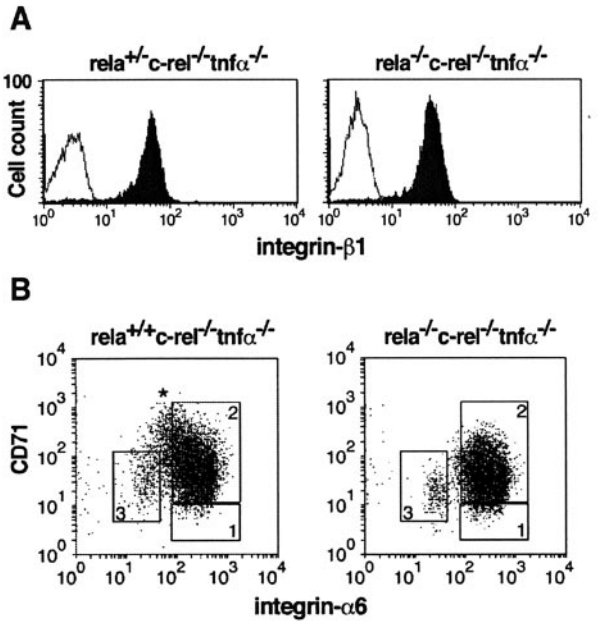


FIG. 5. Flow cytometric analysis of epidermal basal cells lacking c-rel and RelA. Basal keratinocytes from E18 control (*rela*$^{+/-}$ c-*rel*$^{-/-}$ *tnf*$\alpha^{-/-}$) and mutant (*rela*$^{-/-}$ c-*rel*$^{-/-}$ *tnf*$\alpha^{-/-}$) fetuses were stained with a fluorescein isothiocyanate-conjugated anti-integrin-β1(shaded histogram) or control anti-CD4 (open histogram) antibody (A). (B) Two-color fluorescence-activated cell sorting analysis was performed by staining with fluorescein isothiocyanate-conjugated anti-integrin-α6 antibody and phycoerythrin-conjugated anti-CD71 antibody. Three phenotypically distinct populations were identified by flow cytometry: quiescent stem cells, α6$^{hi}$ CD71$^{lo}$ (gate 1); TA cells, α6$^{hi}$ CD71$^{hi}$ (gate 2); and postmitotic differentiating cells, α6$^{lo}$ CD71$^{hi}$ (gate 3). Cells with high CD71 expression in the control profile (asterisk) were markedly reduced in the mutant.

To assess if the impaired epidermal development in the absence of c-rel and RelA might be due to reduced numbers of epidermal stem cells and TA cells, equivalent areas of skin (0.5 cm$^2$) were removed from the flanks of E18 control and mutant fetuses, and epidermal basal cells were isolated by protease treatment. Comparable numbers of basal cells were isolated from control *rela*$^{+/-}$ c-*rel*$^{-/-}$ *tnf*$\alpha^{-/-}$ ($7.3 \times 10^5 \pm 1.3 \times 10^5$, $n = 4$) and mutant *rela*$^{-/-}$ c-*rel*$^{-/-}$ *tnf*$\alpha^{-/-}$ ($6.3 \times 10^5 \pm 1.8 \times 10^5$, $n = 3$) embryonic skin. Flow cytometric analysis of these cells stained with anti-β1-integrin antibody (Fig. 5A) demonstrated equivalent patterns of integrin-β1 expression in control and mutant epidermal populations, indicating that stem and TA cell numbers were comparable. This conclusion was generally reinforced by the staining profiles for integrin α6 and CD71 (Fig. 5B). However, in the mutant, a minor population of integrin α6$^{hi}$ CD71$^{hi}$ TA cells was markedly reduced. This population probably represents cells in transition from TA cells to differentiating keratinocytes (58). Reduced numbers of this population in *rela*$^{-/-}$ c-*rel*$^{-/-}$ *tnf*$\alpha^{-/-}$ skin is consistent with fewer cells leaving the basal layer, a notion supported by the presence of fewer postmitotic differentiating cells in the *rela*$^{-/-}$ c-*rel*$^{-/-}$ *tnf*$\alpha^{-/-}$ epidermis (gate 3) (Fig. 5B).

**Epidermal basal cells lacking c-rel and RelA exhibit a cell cycle defect.** Although normal numbers of keratinocyte pro-

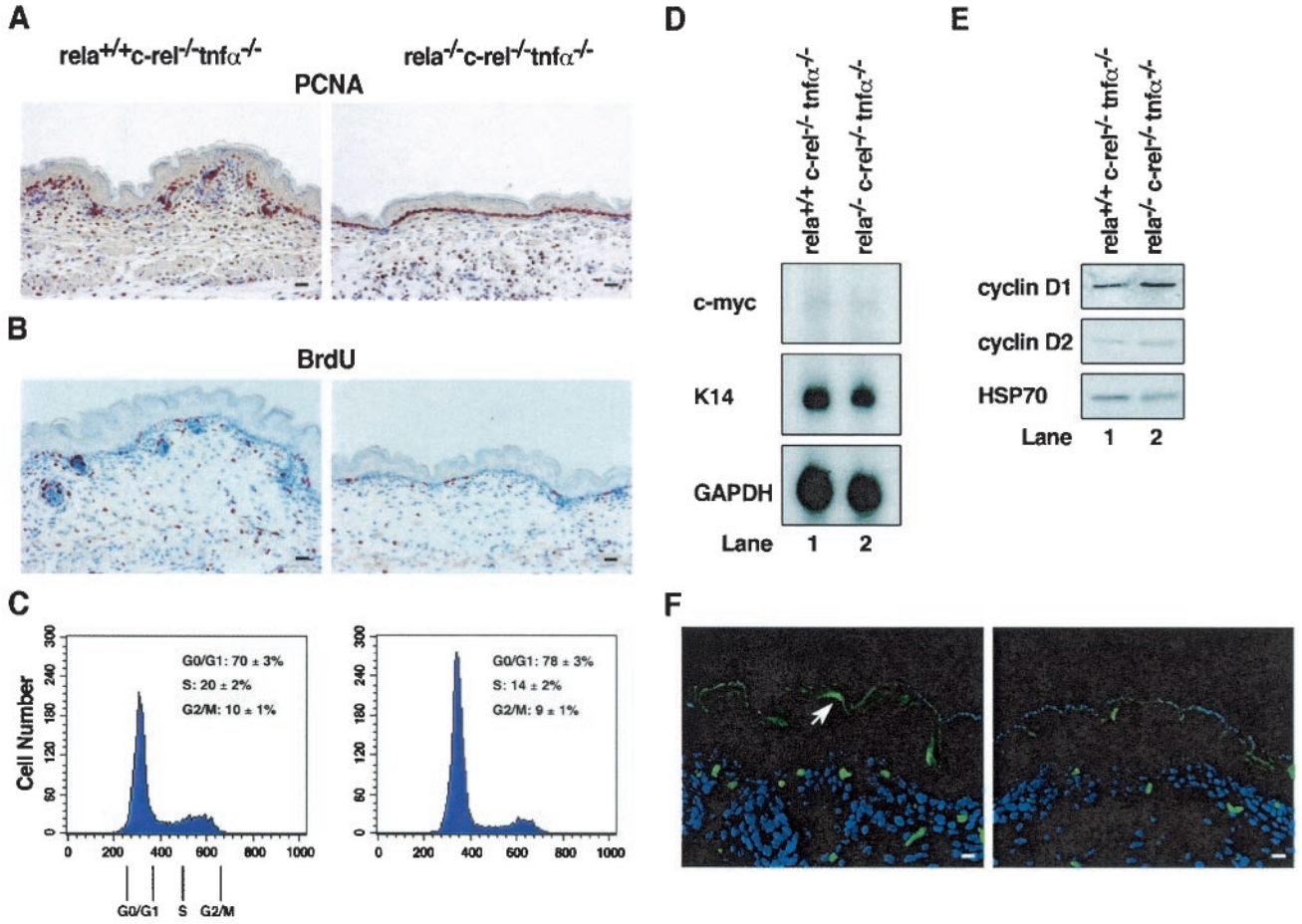


FIG. 6. Cell cycle defect in TA cells lacking RelA and c-rel. Immunohistochemical staining of control (*rela*$^{+/+}$ c-*rel*$^{-/-}$ *tnf*$\alpha^{-/-}$) and mutant (*rela*$^{-/-}$ c-*rel*$^{-/-}$ *tnf*$\alpha^{-/-}$) skin sections for (A) PCNA expression and (B) bromodeoxyuridine incorporation. Bar, 425 μm. (C) Control and mutant TA cells ($\alpha6^{hi}$ CD71$^{hi}$) were purified by fluorescence-activated cell sorting based on the gates shown in Fig. 5B (gate 2), and the DNA content was determined by propidium iodide staining of viable cells. Profiles are representative of six control and six mutant fetuses from six independent experiments. Mod-Fit software was used to determine the proportion of TA in $G_0/G_1$, S, and $G_2/M$. (D) c-*myc* mRNA expression is normal in *rela*$^{-/-}$ c-*rel*$^{-/-}$ *tnf*$\alpha^{-/-}$ keratinocytes. Total RNA isolated from *rela*$^{+/+}$ c-*rel*$^{-/-}$ *tnf*$\alpha^{-/-}$ (lane 1) and mutant *rela*$^{-/-}$ c-*rel*$^{-/-}$ *tnf*$\alpha^{-/-}$ (lane 2) keratinocytes was subjected to Northern blot analysis with radiolabeled cDNA probes for murine c-*myc*, keratin-14, and glyceraldehhyde-3-phosphate dehydrogenase (GAPDH). (E) Cyclin D1 and D2 expression in *rela*$^{-/-}$ c-*rel*$^{-/-}$ *tnf*$\alpha^{-/-}$ keratinocytes. Total protein extracts from *rela*$^{+/+}$ c-*rel*$^{-/-}$ *tnf*$\alpha^{-/-}$ (lane 1) and mutant *rela*$^{-/-}$ c-*rel*$^{-/-}$ *tnf*$\alpha^{-/-}$ (lane 2) keratinocytes were subjected to Western blotting. Filters were sequentially probed with antibodies for cyclin D1, cyclin D2, and HSP70. (F) Control (*rela*$^{+/+}$ c-*rel*$^{-/-}$ *tnf*$\alpha^{-/-}$) (left panel) and mutant (*rela*$^{-/-}$ c-*rel*$^{-/-}$ *tnf*$\alpha^{-/-}$) (right panel) dorsal skin was analyzed by TUNEL staining. Note the apoptotic bodies (arrow) in the stratum granulosum. Bar, 225 μm.

genitors are present in the epidermis of E18 *rela*$^{-/-}$ c-*rel*$^{-/-}$ *tnf*$\alpha^{-/-}$ mice and are able to undergo terminal differentiation, a thinner suprabasal layer in the mutant fetus indicated that epidermal differentiation was abnormal. Since Rel/NF-κB is required for lymphocyte (12) and fibroblast (19, 22) proliferation, one plausible explanation for the reduced thickness of the epidermis was that a defect in cell division might influence the rate at which TA cells undergo terminal differentiation.

Cell division within the mutant epidermis was initially examined in fetal skin sections by immunostaining for proliferating nuclear cell antigen (PCNA) expression, a marker of cells in the late $G_1$ and S phases of the cell cycle (Fig. 6A). In control skin, only some basal cells were PCNA positive, a finding consistent with a nonsynchronous population of cells at different stages of the cell cycle. PCNA-positive cells were also detected in developing hair follicles and the stratum spinosum. In contrast, the majority of cells in the mutant basal layer were PCNA positive, but few positive cells were observed in the suprabasal region. To distinguish between basal keratinocytes in $G_1$ and S phases, bromodeoxyuridine incorporation studies were performed with day 18 fetuses (Fig. 6B). In control skin, bromodeoxyuridine was incorporated by cells within hair follicles and by basal keratinocytes, with ≈20% of basal cells being bromodeoxyuridine positive. However, in *rela*$^{-/-}$ c-*rel*$^{-/-}$ *tnf*$\alpha^{-/-}$ fetal skin, only ≈9% of basal cells were bromodeoxyuridine positive.

The combined PCNA expression and bromodeoxyuridine incorporation studies indicated that the transition from $G_1$ to S phase may be impaired in mutant epidermal basal cells. This was confirmed by measuring the DNA content of fluorescence-activated cell sorting-sorted TA cells (integrin $\alpha6^{hi}$ CD71$^{hi}$) isolated from E18 control and mutant fetuses. A typical set of data is shown in Fig. 6C. Consistent with the findings for bromodeoxyuridine incorporation, only 12 to 14% of mutant

TA cells were in S phase, compared with 20 to 22% of control TA cells. Moreover, whereas comparable proportions of control and mutant TA cells were in $G_2$/M (10% versus 9%, respectively), the reduced frequency of mutant TA cells in S phase was accompanied by a corresponding increase of cells in $G_0/G_1$ (70 versus 78% for control and mutant TA cells, respectively).

These results indicated that TA cells lacking c-rel and RelA exhibit a delay in $G_1$/S-phase progression. This finding, coupled with the reduced size of mutant c-*rel*$^{-/-}$ *rela*$^{-/-}$ *tnf*$\alpha^{-/-}$ TA cells, indicated that impaired cell growth may underlie the cell cycle defect. In eukaryotic cells, growth is thought to proceed throughout $G_1$ until a threshold is reached, at which point levels of certain cellular components that function as indicators of cell size are sufficient to trigger entry into S phase (7). Mitogen-induced B-cell growth is at least in part controlled by the Rel/NF-κB-dependent induction of c-*myc* transcription (17). Levels of c-*myc* mRNA expression, however, were comparable in control and mutant epidermal TA cells (Fig. 6D). The levels of cyclins D1 and D2, important regulators of $G_1$ that are also known targets of Rel/NF-κB (19, 22, 25), were also similar in control and mutant TA cells (Fig. 6E), as were the cdk inhibitors p21 and p27 (results not shown). This indicates that the impaired expression of an unknown Rel/NF-κB target gene is responsible for the $G_1$ growth defect observed in c-*rel*$^{-/-}$ *rela*$^{-/-}$ *tnf*$\alpha^{-/-}$ epidermal basal cells.

During B-cell proliferation, Rel/NF-κB regulates $G_1$/S-phase progression and promotes cell survival (16). To assess whether increased apoptosis accompanied impaired c-*rel*$^{-/-}$ *rela*$^{-/-}$ *tnf*$\alpha^{-/-}$ TA cell division, TUNEL staining was performed on sections of control and mutant fetal skin (Fig. 6F). Mutant epidermis did not have abnormally increased numbers of TUNEL-positive cells. Dying cells were largely confined to the stratum granulosum of both control and mutant skin, a region of the epidermis in which keratinocytes undergo enucleation. Thus, the impaired cell cycle regulation of basal cells lacking RelA and c-rel does not cause abnormally elevated cell death.

**Keratinocytes lacking c-rel and RelA fail to form colonies in culture.** To examine if the c-*rel*$^{-/-}$ *rela*$^{-/-}$ *tnf*$\alpha^{-/-}$ TA cell cycle defect observed in vivo influenced the capacity of these cells to form keratinocyte colonies in culture, we performed colony formation analysis with E18 control and mutant keratinocytes. Whereas numerous keratin-14-positive colonies were evident in 7-day cultures of control cells, c-*rel*$^{-/-}$ *rela*$^{-/-}$ *tnf*$\alpha^{-/-}$ keratinocytes generated only a few colonies that comprised three to four cells (Fig. 7A). The defect in keratinocyte colony formation was only observed in the combined absence of RelA and c-rel (Fig. 7B) and coincided with high levels of cell death (results not shown).

**Hyperproliferation of *rela*$^{-/-}$ c-*rel*$^{-/-}$ *tnf*$\alpha^{-/-}$ embryonic skin grafted onto *rag-1*$^{-/-}$ mice.** In order to examine the consequences of the loss of RelA and c-rel for adult murine skin, E18 control and mutant skin was transplanted onto immunocompromised *rag-1*$^{-/-}$ mice. The clinical appearance of a typical set of skin grafts over a 4-week period is shown in Fig. 8A. Two weeks posttransplantation, the appearance of control donor skin was comparable to that of mutant donor skin. After 3 weeks there was abundant hair growth in control grafts. Only sparse hair growth was present in the mutant skin, which by 4 weeks had disappeared and was accompanied by scaling of the skin.

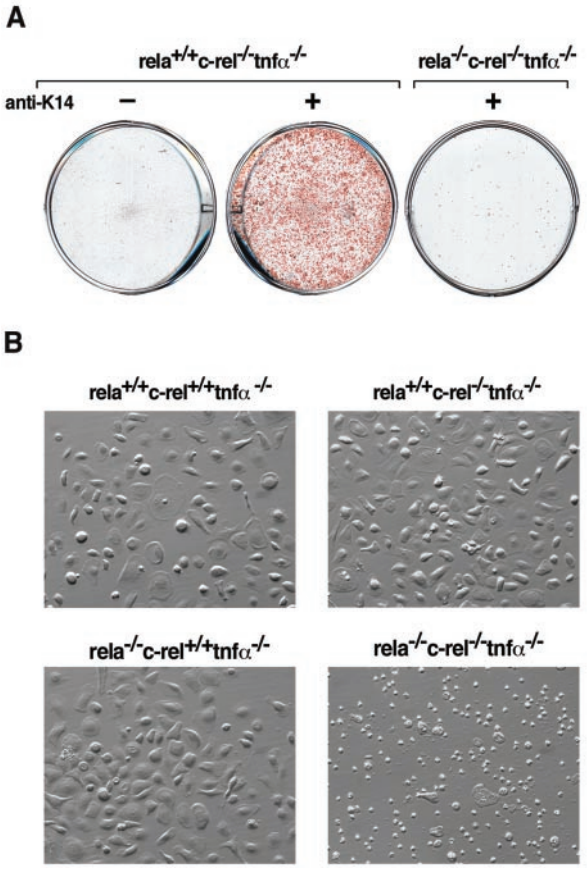


FIG. 7. Keratinocytes lacking RelA and c-rel fail to form colonies in culture. Equivalent numbers of viable keratinocytes ($10^6$) were grown for 7 days. (A) Control (*rela*$^{+/+}$ c-*rel*$^{-/-}$ *tnf*$\alpha^{-/-}$) and mutant (*rela*$^{-/-}$ c-*rel*$^{-/-}$ *tnf*$\alpha^{-/-}$) keratinocyte cultures were stained with anti-keratin-14 (+) or isotype-matched negative-control (−) antibodies. (B) Keratinocytes of differing genotypes (*rela*$^{+/+}$ c-*rel*$^{+/+}$ *tnf*$\alpha^{-/-}$, *rela*$^{+/+}$ c-*rel*$^{-/-}$ *tnf*$\alpha^{-/-}$, *rela*$^{-/-}$ c-*rel*$^{+/+}$ *tnf*$\alpha^{-/-}$, and *rela*$^{-/-}$ c-*rel*$^{-/-}$ *tnf*$\alpha^{-/-}$) are shown by phase contrast.

Histology revealed a striking difference in the architecture of the control and mutant skin grafts. After 4 weeks, control grafts had an epidermis with a well-aligned basal cell layer, one to two cells thick (Fig. 8Bi). The mutant graft exhibited extensive epidermal hyperplasia, hyperkeratosis, focal parakeratosis, and corneal pustules with a granulocytic infiltrate and necrosis (Fig. 8Bii). The mutant epidermis was abnormally thick (six to seven cell layers) with many hyperchromatic cells in the basal layer and a compacted stratum corneum (Fig. 8Ci and Cii). The dermis in the mutant graft was extensively infiltrated with immune cells, eosinophils being most prominent (Fig. 8Ci and Cii). Interestingly, numerous abnormal hair follicles were present in the mutant skin graft that consisted of enlarged sebaceous glands at the base of the follicles (Fig. 8Bii). Staining for melanin granules revealed extensive hyperpigmentation at the dermal-epidermal junction of the mutant graft (Fig. 8Civ), whereas in control grafts, melanin deposits were confined to the reticular dermis (data not shown) and hair bulbs (Fig. 8Ciii). Antibody staining for keratin-6, a marker of prolifera-

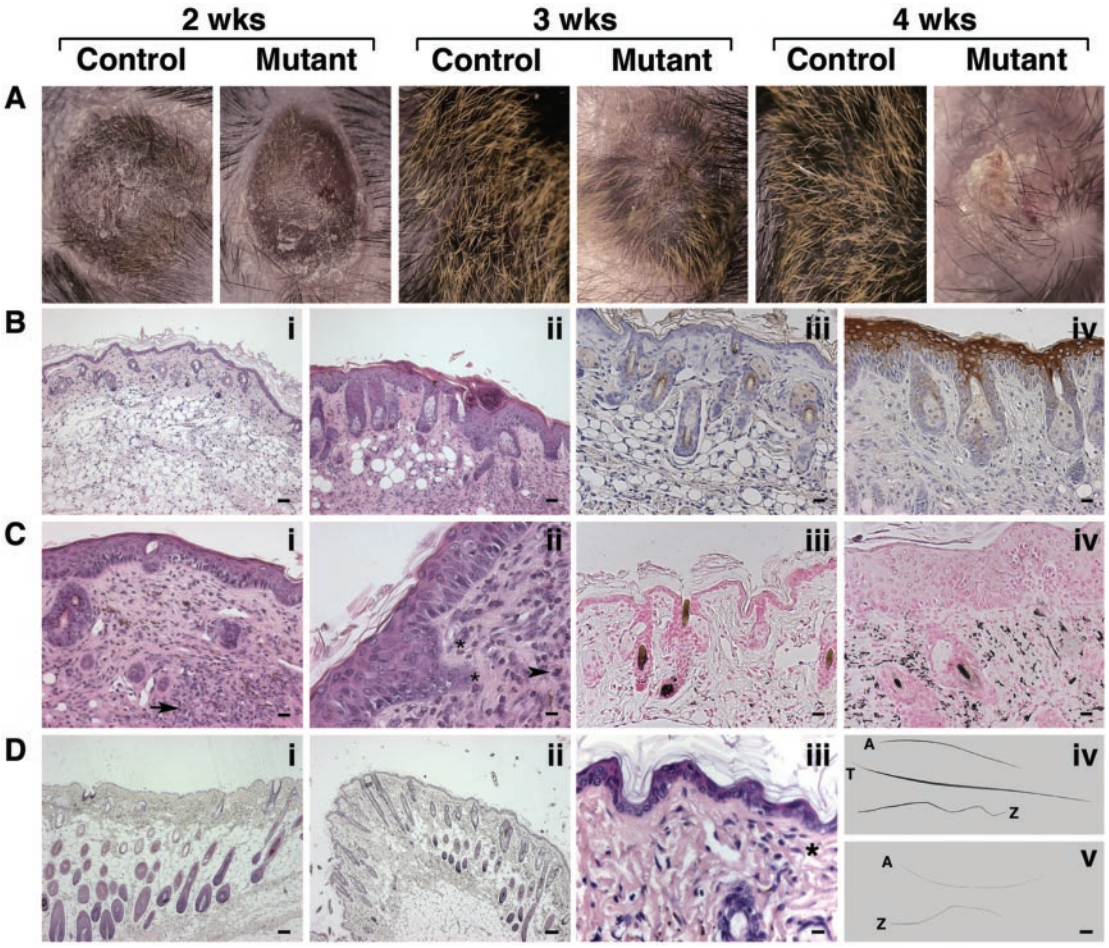


FIG. 8. RelA/c-rel-deficient skin grafts develop TNF-α-dependent epidermal hyperplasia. Skin from E18 control (*rela*$^{+/+}$ c-*rel*$^{-/-}$ *tnf*α$^{-/-}$) and mutant (*rela*$^{-/-}$ c-*rel*$^{-/-}$ *tnf*α$^{-/-}$) fetuses was grafted onto C57BL/6 *rag-1*$^{-/-}$ mice (A, Bi to iv, and Ci to iv) or C57BL/6 *rag-1*$^{-/-}$ *tnf*α$^{-/-}$ mice (Di to v). (A) Appearance of representative donor skin grafts over a 4-week period. (B and C) Histological analysis of skin grafts on C57BL/6 *rag-1*$^{-/-}$ recipients is representative of four control and three mutant skin grafts. H&E-stained sections from control (Bi) and mutant (Bii) skin grafts were analyzed under low power at 4 weeks. Bar, 1,600 μm. Staining for keratin-6 was confined to hair follicles in the control graft (Biii) and the epidermis in the mutant graft (Biv). Bar, 425 μm. High-power analysis of H&E-stained sections revealed pockets of dermal infiltrate (arrow) in the mutant graft (Ci) that were mostly eosinophilic (asterisks) and granulocytic (arrowhead) (Cii). Bar, 225 μm. Note red cytoplasmic staining of eosinophils. Pearl staining for melanin on paraffin sections of control (Ciii) and mutant (Civ) grafts. (D) Skin grafts on C57BL/6 *rag-1*$^{-/-}$ *tnf*α$^{-/-}$ recipients at 4 weeks is representative of three control and three mutant grafts. H&E-stained sections from control (Di) and mutant (Dii) grafts were analyzed at low power. Bar, 1,600 μm. Some dermal infiltrate (fibroblasts and macrophages; asterisks) was observed in the mutant graft (Diii). Three major hair types (tyrlotrich, awl, and zigzag) were observed in the control graft (Div), while only two (awl and zigzag) were evident in the mutant graft (Dv). Note that the mutant hairs are thinner.

tive skin conditions, confirmed that the increased thickness of the epidermis in the mutant skin graft was the result of keratinocyte proliferation (Fig. 8Biv), whereas keratin-6 staining was confined to hair follicles in control skin grafts (Fig. 8Biii).

**Hyperproliferative state of *rela*$^{-/-}$ c-*rel*$^{-/-}$ *tnf*α$^{-/-}$ embryonic skin grafts is dependent on TNF-α.** Hyperproliferation of *rela*$^{-/-}$ c-*rel*$^{-/-}$ *tnf*α$^{-/-}$ epidermal cells in the skin grafts was associated with an immune infiltration, suggesting that this condition may be due in part to these cells secreting inflammatory mediators. Consistent with this possibility was the recent finding that skin inflammation in mice arising from the conditional deletion of IKKβ in epidermal basal cells could be prevented by loss of TNFR1 (44). However, as TNFR1 binds the inflammatory mediators TNF-α and lymphotoxin (LTα) (51), it was unclear if this inflammation was caused by one or both cytokines. Consequently, *rela*$^{-/-}$ c-*rel*$^{-/-}$ *tnf*α$^{-/-}$ E18 fetal skin was grafted onto *rag*$^{-/-}$ *tnf*α$^{-/-}$ recipients to determine if the hyperproliferative state was TNF-α dependent.

Four weeks posttransplantation, mutant grafts showed no evidence of the hyperproliferative condition (Fig. 8Di and Dii). In mutant grafts, the epidermis was two to three cell layers thick, and hair follicles were of relatively normal appearance. The extensive infiltration of leukocytes was markedly reduced, although some macrophages and granulocytic foci were still seen in the dermis (Fig. 8Diii and data not shown). Despite the hyperproliferative condition being eliminated in the absence of TNF-α, a higher frequency of PCNA-positive basal cells was still detected in the mutant graft (results not shown). This suggests that the cell cycle defect seen in mutant fetal skin may still afflict mutant epidermal cells in an adult environment.

## DISCUSSION

Various studies indicate that the Rel/NF-κB signaling pathway is important for skin development and function. However, a wide spectrum of skin phenotypes in different experimental models of perturbed Rel/NF-κB function has generated confusion about the precise role of this pathway in the skin (30). Discrepancies between these models are likely to result from functional redundancy within the pathway coupled with the selective disruption of Rel/NF-κB regulation within discrete compartments of the skin. In an attempt to examine the overall role of Rel/NF-κB transcription factors in skin development, mice lacking RelA plus c-rel or NF-κB1 were bred onto a *tnfα*$^{-/-}$ background. With this strategy, RelA and c-rel were shown to be the critical Rel/NF-κB proteins necessary for normal skin development. During embryogenesis, the combined loss of RelA and c-rel resulted in defective hair follicle morphogenesis, reduced basal keratinocyte division and impaired epidermal cell differentiation. Experiments involving *rela*$^{-/-}$ c-*rel*$^{-/-}$ *tnfα*$^{-/-}$ fetal skin grafts also revealed a key role for RelA and c-rel in suppressing innate immune-mediated epidermal inflammation.

The results presented here establish that c-rel and RelA regulate skin development in a redundant manner. The overlapping functions of these transcription factors in the skin were unexpected. RelA expression is thought to be ubiquitous (3), whereas prior studies had indicated that c-rel expression was restricted to hematopoietic cells (3). The findings presented here show that c-*rel* is also expressed in fetal epidermis and hair placodes, sites in the skin that exhibit the defects in basal cell proliferation and hair follicle formation seen in *rela*$^{-/-}$ c-*rel*$^{-/-}$ *tnfα*$^{-/-}$ embryos. This points to a direct role for c-rel in the development and function of these structures in the skin. In contrast, the combined absence of NF-κB1 and RelA, transcription factors expressed in basal epidermal cells (52), had no significant effect on epidermal or hair follicle development.

A comparison of the skin defects afflicting mice lacking c-rel plus RelA or various IKK components highlights phenotypic similarities between the *rela*$^{-/-}$ c-*rel*$^{-/-}$ *tnfα*$^{-/-}$, *ikkβ*$^{-/-}$, and *ikkγ*$^{-/-}$ mice. An absence of IKKγ, like the loss of c-rel plus RelA, causes defects in hair follicle formation, while innate immune-mediated inflammation is a phenotype shared with IKKβ and IKKγ deficiencies (39, 44, 49). The skin abnormalities in the absence of c-rel and RelA do not resemble those seen in *ikkα*$^{-/-}$ mice, a finding consistent with the *ikkα*$^{-/-}$ defects being Rel/NF-κB independent (24). These observations reinforce the notion that c-rel and RelA are the key downstream effectors of IKKβ and IKKγ function in skin development. Interestingly, defects in neither epidermal structure nor differentiation have been reported in IKKβ- or IKKγ-deficient embryos (39, 49). This inconsistency with the phenotype seen in the *rela*$^{-/-}$ c-*rel*$^{-/-}$ *tnfα*$^{-/-}$ mice indicates that both kinases function redundantly during epidermal differentiation.

The impaired hair follicle morphogenesis and defective tooth development observed in *rela*$^{-/-}$ c-*rel*$^{-/-}$ *tnfα*$^{-/-}$ embryos resemble the phenotype of *tabby* and *downless* mice (21, 41, 51), and a group of human genetic disorders termed hypohydrotic ectodermal dysplasia. These mouse and most human hypohydrotic ectodermal dysplasia disorders arise from mutations in the genes for ectodysplasin (EDA) and ectodysplasin A receptor (EDAR), which encode TNF-like ligand and TNF receptor superfamily members, respectively (21, 31, 41, 42, 55). Importantly, EDA/EDAR signaling activates NF-κB in transfected cells (64). Moreover, mice in which mutant IκBα is ubiquitously expressed exhibit a phenotype identical to that of *tabby* and *downless* mutants (50).

EDAR expression is normally detected in the placodes and bulbs of all four hair types during their sequential morphogenesis (34). The first wave of hair follicle development (tylotrich/guard hair), which depends on EDA/EDAR signaling (34), is absent at E16 in the *rela*$^{-/-}$ c-*rel*$^{-/-}$ *tnfα*$^{-/-}$ mice. By E17, hair placodes were detected in the *rela*$^{-/-}$ c-*rel*$^{-/-}$ *tnfα*$^{-/-}$ mutants, a developmental phase that coincides with the initiation of awl hair formation. Consistent with RelA/ c-rel signaling being required for tylotrich but not awl or zigzag hair types, only awl and zigzag hair was found in the *rela*$^{-/-}$ c-*rel*$^{-/-}$ *tnfα*$^{-/-}$ skin engrafted onto *rag-1*$^{-/-}$ *tnfa*$^{-/-}$ mice (Fig. 8Div and Dv). This finding is also consistent with Wnt rather than EDA/EDAR signaling being necessary for initiating awl follicle formation (8, 34). Although awl and zigzag hair types develop in the absence of c-rel and RelA, these hairs are much thinner than those from control grafts. This indicates that c-rel and RelA are required not only for the initiation of tylotrich hair follicle formation, but also for normal development of *awl* and *zigzag* hair.

Here we show that *rela*$^{-/-}$ c-*rel*$^{-/-}$ *tnfα*$^{-/-}$ fetuses have a thinner epidermis. Although this coincides with a reduction in the size of the suprabasal layer, the expression of markers for various distinct postmitotic epidermal layers indicates that terminal keratinocyte differentiation still proceeds in the correct sequential manner in the absence of c-rel and RelA. This conclusion is supported by the presence of a functional cornified barrier in *rela*$^{-/-}$ c-*rel*$^{-/-}$ *tnfα*$^{-/-}$ fetuses. Normal numbers of epidermal stem cells and their progeny, the TA cells in *rela*$^{-/-}$ c-*rel*$^{-/-}$ *tnfα*$^{-/-}$ skin, indicate that this epidermal defect is unlikely to involve impaired stem cell differentiation. Instead, these observations suggest that a reduced rate of keratinocyte differentiation is the likely cause of the thinner epidermis.

While we cannot exclude a direct role for c-rel and RelA in epidermal suprabasal cell differentiation, the basal keratinocyte cell cycle defect offers an alternative explanation for the thinner *rela*$^{-/-}$ c-*rel*$^{-/-}$ *tnfα*$^{-/-}$ fetal epidermis. Keratinocytes normally complete a limited number of divisions before exiting the cell cycle and migrating to the surface of the skin while undergoing terminal differentiation. With fewer *rela*$^{-/-}$ c-*rel*$^{-/-}$ *tnfα*$^{-/-}$ basal keratinocytes in S phase, a slower rate of division is likely to result in fewer basal cells being available to exit the cell cycle and differentiate.

The finding that a higher proportion of mutant keratinocytes were in $G_0/G_1$ indicates that the cell cycle defect is in $G_1$. Consistent with this conclusion was the smaller than normal size of *rela*$^{-/-}$ c-*rel*$^{-/-}$ *tnfα*$^{-/-}$ basal cells, a characteristic indicative of a growth defect. This finding for the epidermal keratinocyte cell cycle closely parallels the function of Rel/NF-κB in B cells. c-rel and NF-κB1 regulate mitogen-induced B-cell growth in $G_1$ by inducing c-*myc* transcription (17). Despite a common role for Rel/NF-κB family members in controlling lymphocyte and keratinocyte growth, c-*myc* expression

is normal in *rela*$^{-/-}$ c-*rel*$^{-/-}$ *tnf*$\alpha^{-/-}$ keratinocytes. This indicates that c-rel and RelA control a different gene necessary for keratinocyte growth. Although TNF-α has not been shown to regulate cell growth, currently we are unable to rule out the possibility that an absence of TNF-α activity on a *rela*$^{-/-}$ c-*rel*$^{-/-}$ background contributes to the defect in cell cycle entry.

In contrast to the modest defect in keratinocyte division observed in *rela*$^{-/-}$ c-*rel*$^{-/-}$ *tnf*$\alpha^{-/-}$ fetuses, when E18 *rela*$^{-/-}$ c-*rel*$^{-/-}$ *tnf*$\alpha^{-/-}$ basal keratinocytes were cultured under conditions that normally promote extensive proliferation, these cells failed to divide in culture and instead underwent apoptosis. It remains to be determined if the death of *rela*$^{-/-}$ c-*rel*$^{-/-}$ *tnf*$\alpha^{-/-}$ keratinocytes in vitro is a direct consequence of impaired growth or due to another defect, such as the failure of these cells to adhere to plastic dishes. In vivo, the degree of cell death among embryonic *rela*$^{-/-}$ c-*rel*$^{-/-}$ *tnf*$\alpha^{-/-}$ keratinocytes was not elevated above normal levels, indicating that their survival is regulated independently of these transcription factors. This differs from B cells, where c-rel promotes both cell division and survival through the regulation of distinct target genes (18).

Due to the death of newborn *rela*$^{-/-}$ c-*rel*$^{-/-}$ *tnf*$\alpha^{-/-}$ mice, mutant embryonic skin was grafted onto immunocompromised *rag-1*$^{-/-}$ recipients to assess the longer-term consequences of the combined RelA/c-rel deficiency. Unlike the hypoproliferative status of basal keratinocytes in the *rela*$^{-/-}$ c-*rel*$^{-/-}$ *tnf*$\alpha^{-/-}$ fetus, mutant fetal skin transplants were characterized by basal cell hyperplasia and immune-mediated inflammation. The histopathology associated with the *rela*$^{-/-}$ c-*rel*$^{-/-}$ *tnf*$\alpha^{-/-}$ skin grafts bore a striking resemblance to the skin phenotype of female *ikk*$\gamma^{+/-}$ mice, an animal model for the human X-linked disorder incontinentia pigmenti (54). Female *ikk*$\gamma^{+/-}$ mice develop a severe dermatopathy that comprises an epidermal hyperplasia, hyperkeratosis, and focal parakeratosis, with an infiltration of pustule-carrying granules and hyperpigmentation near the epidermal-dermal junction (39, 49). Hair loss and tooth defects are also associated with incontinentia pigmenti (2). As it is not uncommon to observe patients with the combined symptoms of hypohydrotic ectodermal dysplasia and incontinentia pigmenti (2), a characteristic shared with the *rela*$^{-/-}$ c-*rel*$^{-/-}$ *tnf*$\alpha^{-/-}$ deficiency, our findings indicate that it is the inability to activate RelA and c-rel that accounts for the defects seen in these patients.

The absence of basal keratinocyte hyperproliferation in *rela*$^{-/-}$ c-*rel*$^{-/-}$ *tnf*$\alpha^{-/-}$ skin grafted onto *rag-1*$^{-/-}$ *tnf*$\alpha^{-/-}$ recipients coincided with an absence of eosinophilia and markedly reduced leukocyte infiltration into the graft. Prevention of this pathology in the mutant graft by blocking TNF-α signaling indicates that the proliferative skin disorder may be driven by inflammatory mediators produced by the innate immune system. This inflammation resembles that recently reported for mice in which IKKβ was selectively deleted in keratin-14-expressing cells (44). Collectively, these data indicate that c-rel and RelA are the downstream effectors of the IKKβ/IKKγ-mediated suppression of epidermal inflammation.

The mechanism by which the IKKβ/IKKγ/c-rel/RelA axis of the Rel/NF-κB pathway suppresses immune-mediated inflammation within the skin remains to be determined. Perhaps epidermal cells lacking c-rel and RelA secrete inflammatory mediators or chemokines that lead to leukocyte recruitment and activation. Although Rel/NF-κB signaling has a well-established role in leukocytes as a positive regulator of cytokine transcription (15), in other cell types, such as keratinocytes, this pathway may suppress cytokine and chemokine expression. Such a model is consistent with c-rel functioning as a positive or negative regulator of specific cytokine expression in a cell type-dependent context (13).

It remains unclear why keratinocytes would adopt a strategy in which immune activation requires the inhibition of Rel/NF-κB. One intriguing possibility is that activating the innate immune system within the skin by inhibiting c-rel and RelA in keratinocytes represents a mechanism to combat viruses that have evolved mechanisms to shut down or circumvent the Rel/NF-κB signaling pathway (48). Collectively, the findings presented here indicate that the role of the c-rel and RelA transcription factors in the skin is multifaceted, serving to regulate the development of different skin structures during embryogenesis and to control the innate immune system in a postembryonic environment.

## ACKNOWLEDGMENTS

We thank D. Baltimore and J. Sedgwick (DNAX) for mice, A. Strasser for critically reading the manuscript, K. Brown and J. Merryfull for animal husbandry, M. Thomson for technical assistance, and S. Mihalovic for histological services.

This work was supported by the National Health and Medical Research Council of Australia and by the Thomas William Francis and Violet Coles Trust.

## REFERENCES

1. **Alcamo, E., J. P. Mizgerd, B. H. Horwitz, R. Bronson, A. A. Beg, M. Scott, C. M. Doerschuk, R. O. Hynes, and D. Baltimore.** 2001. Targeted mutation of TNF receptor I rescues the RelA-deficient mouse and reveals a critical role for NF-kappaB in leukocyte recruitment. J. Immunol. **167:**1592–1600.
2. **Aradhya, S., and D. L. Nelson.** 2001. NF-kappaB signaling and human disease. Curr. Opin. Genet. Dev. **11:**300–306.
3. **Baldwin, A. S., Jr.** 1996. The NF-kappa B and I kappa B proteins: new discoveries and insights. Annu. Rev. Immunol. **14:**649–683.
4. **Barton, D., H. HogenEsch, and F. Weih.** 2000. Mice lacking the transcription factor RelB develop T cell-dependent skin lesions similar to human atopic dermatitis. Eur. J. Immunol. **30:**2323–2332.
5. **Beg, A. A., W. C. Sha, R. T. Bronson, and D. Baltimore.** 1995. Constitutive NF-kappa B activation, enhanced granulopoiesis, and neonatal lethality in I kappa B alpha-deficient mice. Genes Dev. **9:**2736–2746.
6. **Beg, A. A., W. C. Sha, R. T. Bronson, S. Ghosh, and D. Baltimore.** 1995. Embryonic lethality and liver degeneration in mice lacking the RelA component of NF-kappa B. Nature **376:**167–170.
7. **Conlon, I., and M. Raff.** 1999. Size control in animal development. Cell **96:**235–244.
8. **DasGupta, R., and E. Fuchs.** 1999. Multiple roles for activated LEF/TCF transcription complexes during hair follicle development and differentiation. Development **126:**4557–4568.
9. **Doi, T. S., M. W. Marino, T. Takahashi, T. Yoshida, T. Sakakura, L. J. Old, and Y. Obata.** 1999. Absence of tumor necrosis factor rescues RelA-deficient mice from embryonic lethality. Proc. Natl. Acad. Sci. USA **96:**2994–2999.
10. **Franzoso, G., L. Carlson, L. Xing, L. Poljak, E. W. Shores, K. D. Brown, A. Leonardi, T. Tran, B. F. Boyce, and U. Siebenlist.** 1997. Requirement for NF-kappaB in osteoclast and B-cell development. Genes Dev. **11:**3482–3496.
11. **Fuchs, E., and C. Byrne.** 1994. The epidermis: rising to the surface. Curr. Opin. Genet. Dev. **4:**725–736.
12. **Gerondakis, S., M. Grossmann, Y. Nakamura, T. Pohl, and R. Grumont.** 1999. Genetic approaches in mice to understand Rel/NF-kappaB and IkappaB function: transgenics and knockouts. Oncogene **18:**6888–6895.
13. **Gerondakis, S., A. Strasser, D. Metcalf, G. Grigoriadis, J. Y. Scheerlinck, and R. J. Grumont.** 1996. Rel-deficient T cells exhibit defects in production of interleukin 3 and granulocyte-macrophage colony-stimulating factor. Proc. Natl. Acad. Sci. USA **93:**3405–3409.
14. **Ghosh, S., and M. Karin.** 2002. Missing pieces in the NF-kappaB puzzle. Cell **109**(Suppl.)**:**S81–S96.
15. **Ghosh, S., M. J. May, and E. B. Kopp.** 1998. NF-kappa B and Rel proteins: evolutionarily conserved mediators of immune responses. Annu. Rev. Immunol. **16:**225–260.
16. **Grumont, R. J., I. J. Rourke, and S. Gerondakis.** 1999. Rel-dependent induction of A1 transcription is required to protect B cells from antigen receptor ligation-induced apoptosis. Genes Dev. **13:**400–411.

17. **Grumont, R. J., A. Strasser, and S. Gerondakis.** 2002. B cell growth is controlled by phosphatidylinosotol 3-kinase-dependent induction of Rel/NF-kappaB regulated c-myc transcription. Mol. Cell **10:**1283–1294.
18. **Gugasyan, R., R. Grumont, M. Grossmann, Y. Nakamura, T. Pohl, D. Nesic, and S. Gerondakis.** 2000. Rel/NF-kappaB transcription factors: key mediators of B-cell activation. Immunol. Rev. **176:**134–140.
19. **Guttridge, D. C., C. Albanese, J. Y. Reuther, R. G. Pestell, and A. S. Baldwin, Jr.** 1999. NF-κB controls cell growth and differentiation through transcriptional regulation of cyclin D1. Mol. Cell. Biol. **19:**5785–5799.
20. **Hardman, M. J., P. Sisi, D. N. Banbury, and C. Byrne.** 1998. Patterned acquisition of skin barrier function during development. Development **125:** 1541–1552.
21. **Headon, D. J., and P. A. Overbeek.** 1999. Involvement of a novel Tnf receptor homologue in hair follicle induction. Nat. Genet. **22:**370–374.
22. **Hinz, M., D. Krappmann, A. Eichten, A. Heder, C. Scheidereit, and M. Strauss.** 1999. NF-κB function in growth control: regulation of cyclin D1 expression and $G_0/G_1$-to-S-phase transition. Mol. Cell. Biol. **19:**2690–2698.
23. **Hu, Y., V. Baud, M. Delhase, P. Zhang, T. Deerinck, M. Ellisman, R. Johnson, and M. Karin.** 1999. Abnormal morphogenesis but intact IKK activation in mice lacking the IKKalpha subunit of IkappaB kinase. Science **284:**316–320.
24. **Hu, Y., V. Baud, T. Oga, K. I. Kim, K. Yoshida, and M. Karin.** 2001. IKKalpha controls formation of the epidermis independently of NF-kappaB. Nature **410:**710–714.
25. **Huang, Y., K. Ohtani, R. Iwanaga, Y. Matsumura, and M. Nakamura.** 2001. Direct trans-activation of the human cyclin D2 gene by the oncogene product Tax of human T-cell leukemia virus type I. Oncogene **20:**1094–1102.
26. **Iotsova, V., J. Caamano, J. Loy, Y. Yang, A. Lewin, and R. Bravo.** 1997. Osteopetrosis in mice lacking NF-kappaB1 and NF-kappaB2. Nat. Med. **3:**1285–1289.
27. **Jones, P. H., and F. M. Watt.** 1993. Separation of human epidermal stem cells from transit amplifying cells on the basis of differences in integrin function and expression. Cell **73:**713–724.
28. **Kalinin, A. E., A. V. Kajava, and P. M. Steinert.** 2002. Epithelial barrier function: assembly and structural features of the cornified cell envelope. Bioessays **24:**789–800.
29. **Karin, M.** 1999. How NF-kappaB is activated: the role of the IkappaB kinase (IKK) complex. Oncogene **18:**6867–6874.
30. **Kaufman, C. K., and E. Fuchs.** 2000. It's got you covered. NF-kappaB in the epidermis. J. Cell Biol. **149:**999–1004.
31. **Kere, J., A. K. Srivastava, O. Montonen, J. Zonana, N. Thomas, B. Ferguson, F. Munoz, D. Morgan, A. Clarke, P. Baybayan, E. Y. Chen, S. Ezer, U. Saarialho-Kere, A. de la Chapelle, and D. Schlessinger.** 1996. X-linked anhidrotic (hypohidrotic) ectodermal dysplasia is caused by mutation in a novel transmembrane protein. Nat. Genet. **13:**409–416.
32. **Klement, J. F., N. R. Rice, B. D. Car, S. J. Abbondanzo, G. D. Powers, P. H. Bhatt, C. H. Chen, C. A. Rosen, and C. L. Stewart.** 1996. IκBα deficiency results in a sustained NF-κB response and severe widespread dermatitis in mice. Mol. Cell. Biol. **16:**2341–2349.
33. **Kontgen, F., R. J. Grumont, A. Strasser, D. Metcalf, R. Li, D. Tarlinton, and S. Gerondakis.** 1995. Mice lacking the c-rel proto-oncogene exhibit defects in lymphocyte proliferation, humoral immunity, and interleukin-2 expression. Genes Dev. **9:**1965–1977.
34. **Laurikkala, J., J. Pispa, H. S. Jung, P. Nieminen, M. Mikkola, X. Wang, U. Saarialho-Kere, J. Galceran, R. Grosschedl, and I. Thesleff.** 2002. Regulation of hair follicle development by the TNF signal ectodysplasin and its receptor Edar. Development **129:**2541–2553.
35. **Li, A., P. J. Simmons, and P. Kaur.** 1998. Identification and isolation of candidate human keratinocyte stem cells based on cell surface phenotype. Proc. Natl. Acad. Sci. USA **95:**3902–3907.
36. **Li, E. R., D. M. Owens, P. Djian, and F. M. Watt.** 2000. Expression of involucrin in normal, hyperproliferative and neoplastic mouse keratinocytes. Exp. Dermatol. **9:**431–438.
37. **Li, Q., Q. Lu, J. Y. Hwang, D. Buscher, K. F. Lee, J. C. Izpisua-Belmonte, and I. M. Verma.** 1999. IKK1-deficient mice exhibit abnormal development of skin and skeleton. Genes Dev. **13:**1322–1328.
38. **Li, Q., D. Van Antwerp, F. Mercurio, K. F. Lee, and I. M. Verma.** 1999. Severe liver degeneration in mice lacking the IkappaB kinase 2 gene. Science **284:**321–325.
39. **Makris, C., V. L. Godfrey, G. Krahn-Senftleben, T. Takahashi, J. L. Roberts, T. Schwarz, L. Feng, R. S. Johnson, and M. Karin.** 2000. Female mice heterozygous for IKK gamma/NEMO deficiencies develop a dermatopathy similar to the human X-linked disorder incontinentia pigmenti. Mol. Cell **5:**969–979.
40. **Mann, S. J.** 1962. Prenatal formation of hair follicle types. Anat. Rec. **144:**135–141.
41. **Monreal, A. W., B. M. Ferguson, D. J. Headon, S. L. Street, P. A. Overbeek, and J. Zonana.** 1999. Mutations in the human homologue of mouse dl cause autosomal recessive and dominant hypohidrotic ectodermal dysplasia. Nat. Genet. **22:**366–369.
42. **Monreal, A. W., J. Zonana, and B. Ferguson.** 1998. Identification of a new splice form of the EDA1 gene permits detection of nearly all X-linked hypohidrotic ectodermal dysplasia mutations. Am. J. Hum. Genet. **63:**380–389.
43. **Nakamura, Y., R. J. Grumont, and S. Gerondakis.** 2002. NF-κB1 can inhibit v-Abl-induced lymphoid transformation by functioning as a negative regulator of cyclin D1 expression. Mol. Cell. Biol. **22:**5563–5574.
44. **Pasparakis, M., G. Courtois, M. Hafner, M. Schmidt-Supprian, A. Nenci, A. Toksoy, M. Krampert, M. Goebeler, R. Gillitzer, A. Israel, T. Krieg, K. Rajewsky, and I. Haase.** 2002. TNF-mediated inflammatory skin disease in mice with epidermis-specific deletion of IKK2. Nature **417:**861–866.
45. **Pohl, T., R. Gugasyan, R. J. Grumont, A. Strasser, D. Metcalf, D. Tarlinton, W. Sha, D. Baltimore, and S. Gerondakis.** 2002. The combined absence of NF-kappa B1 and c-rel reveals that overlapping roles for these transcription factors in the B cell lineage are restricted to the activation and function of mature cells. Proc. Natl. Acad. Sci. USA **99:**4514–4519.
46. **Rosenfeld, M. E., L. Prichard, N. Shiojiri, and N. Fausto.** 2000. Prevention of hepatic apoptosis and embryonic lethality in RelA/TNFR-1 double knockout mice. Am. J. Pathol. **156:**997–1007.
47. **Rudolph, D., W. C. Yeh, A. Wakeham, B. Rudolph, D. Nallainathan, J. Potter, A. J. Elia, and T. W. Mak.** 2000. Severe liver degeneration and lack of NF-kappaB activation in NEMO/IKKgamma-deficient mice. Genes Dev. **14:**854–862.
48. **Santoro, M. G., A. Rossi, and C. Amici.** 2003. NF-kappaB and virus infection: who controls whom. EMBO J. **22:**2552–2560.
49. **Schmidt-Supprian, M., W. Bloch, G. Courtois, K. Addicks, A. Israel, K. Rajewsky, and M. Pasparakis.** 2000. NEMO/IKK gamma-deficient mice model incontinentia pigmenti. Mol. Cell **5:**981–992.
50. **Schmidt-Ullrich, R., T. Aebischer, J. Hulsken, W. Birchmeier, U. Klemm, and C. Scheidereit.** 2001. Requirement of NF-kappaB/Rel for the development of hair follicles and other epidermal appendices. Development **128:** 3843–3853.
51. **Sedgwick, J. D., D. S. Riminton, J. G. Cyster, and H. Korner.** 2000. Tumor necrosis factor: a master-regulator of leukocyte movement. Immunol. Today **21:**110–113.
52. **Seitz, C. S., Q. Lin, H. Deng, and P. A. Khavari.** 1998. Alterations in NF-kappaB function in transgenic epithelial tissue demonstrate a growth inhibitory role for NF-kappaB. Proc. Natl. Acad. Sci. USA **95:**2307–2312.
53. **Senftleben, U., Y. Cao, G. Xiao, F. R. Greten, G. Krahn, G. Bonizzi, Y. Chen, Y. Hu, A. Fong, S. C. Sun, and M. Karin.** 2001. Activation by IKKalpha of a second, evolutionary conserved, NF-kappa B signaling pathway. Science **293:**1495–1499.
54. **Smahi, A., G. Courtois, P. Vabres, S. Yamaoka, S. Heuertz, A. Munnich, A. Israel, N. S. Heiss, S. M. Klauck, P. Kioschis, S. Wiemann, A. Poustka, T. Esposito, T. Bardaro, F. Gianfrancesco, A. Ciccodicola, M. D'Urso, H. Woffendin, T. Jakins, D. Donnai, H. Stewart, S. J. Kenwrick, S. Aradhya, T. Yamagata, M. Levy, R. A. Lewis, and D. L. Nelson.** 2000. Genomic rearrangement in NEMO impairs NF-kappaB activation and is a cause of incontinentia pigmenti. The International Incontinentia Pigmenti (IP) Consortium. Nature **405:**466–472.
55. **Srivastava, A. K., J. Pispa, A. J. Hartung, Y. Du, S. Ezer, T. Jenks, T. Shimada, M. Pekkanen, M. L. Mikkola, M. S. Ko, I. Thesleff, J. Kere, and D. Schlessinger.** 1997. The Tabby phenotype is caused by mutation in a mouse homologue of the EDA gene that reveals novel mouse and human exons and encodes a protein (ectodysplasin-A) with collagenous domains. Proc. Natl. Acad. Sci. USA **94:**13069–13074.
56. **Takeda, K., O. Takeuchi, T. Tsujimura, S. Itami, O. Adachi, T. Kawai, H. Sanjo, K. Yoshikawa, N. Terada, and S. Akira.** 1999. Limb and skin abnormalities in mice lacking IKKalpha. Science **284:**313–316.
57. **Tanaka, M., M. E. Fuentes, K. Yamaguchi, M. H. Durnin, S. A. Dalrymple, K. L. Hardy, and D. V. Goeddel.** 1999. Embryonic lethality, liver degeneration, and impaired NF-kappa B activation in IKK-beta-deficient mice. Immunity **10:**421–429.
58. **Tani, H., R. J. Morris, and P. Kaur.** 2000. Enrichment for murine keratinocyte stem cells based on cell surface phenotype. Proc. Natl. Acad. Sci. USA **97:**10960–10965.
59. **Thomas, T., A. K. Voss, K. Chowdhury, and P. Gruss.** 2000. Querkopf, a MYST family histone acetyltransferase, is required for normal cerebral cortex development. Development **127:**2537–2548.
60. **van Hogerlinden, M., B. L. Rozell, L. Ahrlund-Richter, and R. Toftgard.** 1999. Squamous cell carcinomas and increased apoptosis in skin with inhibited Rel/nuclear factor-kappaB signaling. Cancer Res. **59:**3299–3303.
61. **Watt, F. M.** 2001. Stem cell fate and patterning in mammalian epidermis. Curr. Opin. Genet. Dev. **11:**410–417.
62. **Watt, F. M.** 2002. Role of integrins in regulating epidermal adhesion, growth and differentiation. EMBO J. **21:**3919–3926.
63. **Whiteside, S. T., and A. Israel.** 1997. I kappa B proteins: structure, function and regulation. Semin. Cancer Biol. **8:**75–82.
64. **Yan, M., L. C. Wang, S. G. Hymowitz, S. Schilbach, J. Lee, A. Goddard, A. M. de Vos, W. Q. Gao, and V. M. Dixit.** 2000. Two-amino acid molecular switch in an epithelial morphogen that regulates binding to two distinct receptors. Science **290:**523–527.